

Dither signal optimization for multi-agent extremum seeking control

Thiago Lima Silva¹ and Alexey Pavlov¹

Abstract—In this paper we formulate and solve the problem of multi-agent extremum seeking with dither signals optimization. The solution is a distributed perturbation-based extremum-seeking controller with an additional objective of minimizing overall dither signals disturbances for the whole system. In particular, the proposed method dynamically calculates dither signals for individual subsystems to minimize the dither-induced variations in the total input and output of the process. The overall scheme consists of a dither signal optimizer coupled with a least-squares gradient estimator and a distributed synchronization-based process optimizer. Simulation results for an oil production system with multiple gas-lifted wells demonstrate that the proposed controller is capable of optimizing the production process, while minimizing, on the fast time scale, dither-induced variations both in the total input (total gas injection rate) and in the total output (total oil production rate) of the production system.

I. INTRODUCTION

Extremum seeking control (ESC) is a popular model-free optimization method, receiving significant attention from the scientific community in the last two decades, see, e.g. [1], [2], [3], [4], [5], [6], [7], [8].

Extremum seeking control allows one to achieve automatic optimization of steady-state behavior of an unknown plant, where the steady-state behavior is quantified in terms of an a-priori unknown cost function. Optimization is achieved by manipulating inputs through feedback of the plant outputs. Apart from applications to optimization of individual systems, ESC has been applied to optimization of systems consisting of multiple interconnected (over a network of certain topology) subsystems, resulting in a number of publications on distributed Extremum Seeking Control for multi-agent systems [9], [10], [11], [12].

Conceptually, extremum seeking controller consists of the following components:

- Dither signal generator (for perturbation-based ESC) that provides excitation of the nominal input signal for extracting information about the gradient of the unknown cost function.
- Gradient estimator – a block that extracts information on the gradient of the cost function from the available measurements of the inputs and outputs of the system. This block estimates either the gradient itself, or a quantity co-directed with the gradient. Clearly, to be able to extract this information, the inputs must have sufficient variation, which is usually guaranteed by the

dither signal or through the variation of the input by the next block – the steady-state optimizer.

- Steady-state optimizer – a block that, based on the estimated gradient, continuously adjusts the nominal input towards the optimum of the cost function.

All these components can be selected and tuned in different ways to achieve guaranteed convergence to the optimum, desired convergence rate, simplicity of the overall controller, and quality of the steady-state optimization, see, e.g., [5], [13], [8] for gradient estimators, and [2], [14] for optimizer designs.

When it comes to dither signals, previous works focused on their shape, frequency and amplitude. The shape affects the convergence rate of the gradient estimator [6]. Dither signal frequency should be sufficiently high in relation to the dynamics in the gradient estimator, process optimizer and the plant dynamics to guarantee convergence to the optimum through time scales separation between these dynamics [3], [15]. The amplitude should be chosen sufficiently small to be able to extract the essentially local information on the gradient of the cost function. At the same time, it should be large enough to ensure gradient estimation in the presence of noise and other practical limitations. One can also select a dither-free ESC scheme [5] and a scheme with the dither signal vanishing at the optimum [16]. Although the dither-free approaches are very elegant, for optimization and *tracking* of a slowly changing optimum, some kind of dither signal still needs to be employed to track possible changes in the optimum.

The shape, frequency and amplitude are the main degrees of freedom for selection of dither signals in extremum seeking control of *individual* systems. When applying ESC to *multiple* systems, like in distributed ESC for multi-agent systems, there appears a new degree of freedom: coordination of dither signals with respect to each other. For example, for two systems one can choose sine dither signals of the same amplitude and frequency, but shifted in phase, i.e. $d_1(t) = a \sin(\omega t)$ and $d_2(t) = a \sin(\omega t + \varphi)$. Provided that the amplitude and frequency are chosen correctly, these dither signals will work well for gradient estimation in both systems, regardless of the selected phase shift φ , which represents the new degree of freedom. In extremum seeking control of individual systems we are free to select not only arbitrary phases, but also amplitudes within a certain minimal/maximal range without compromising convergence properties of the algorithm. Therefore, in addition to phases we can also use dither signals amplitudes (within a certain range) to coordinate the dither signals.

This new degree of freedom is essential in a number of

*This work is part of the BRU21 research program at NTNU (www.ntnu.edu/bru21)

¹ Thiago Lima Silva and Alexey Pavlov are with the Department of Geoscience and Petroleum, NTNU, 7031 Trondheim, Norway, e-mails: thiago.l.silva@ntnu.no, alexey.pavlov@ntnu.no

potential ESC applications. In particular, in process control applications, large/fast variations in the overall input signal (the sum of all input signals) and/or large/fast variations in the overall output (the sum of all output signals) represent a significant disturbance to the overall process. Such variations may not be compatible with the process limitations or may represent an undesired disturbance for the rest of the process. For our example with two systems, the sum of input variations due to dither signals equals $d_1(t) + d_2(t) = a \sin(\omega t) + a \sin(\omega t + \varphi)$. If the phase shift is chosen to be $\varphi = 0$, the total amplitude will be equal to $2a$. For N systems, the amplitude will be Na . Even though for each individual system a can be chosen small (as is usually done in ESC), the total variation of all dither signals can be prohibitively large. On the other hand, if, for two systems, the phase shift is chosen $\varphi = 180$ deg, we will have $d_1(t) + d_2(t) \equiv 0$, which is definitely an advantage in the above mentioned applications, as it represents no further disturbance to the overall process input.

This simple example demonstrates that optimal (in some sense) coordination of dither signals is important and can be essential for a number of applications of ESC to multi-agent systems. The problem of optimal coordination of dither signals becomes more interesting if one wants to cancel dither-based variations not only in the total input, but also in the total output of the systems, which is also affected by the choice of the dither signals.

In this paper we, firstly, demonstrate, by a motivating example from the petroleum industry, the importance of dither signals optimization for reduction of overall process disturbances. Secondly, we formulate the problem of *dither signals optimization* in distributed ESC, which is a new class of problems within ESC for multi-agent systems. To the best of our knowledge, these problems have neither been formulated nor addressed in the prior literature on ESC (apart from our paper [12], where we briefly discuss this challenge, but only for the input signals). Thirdly, we provide a method that solves the problem of dither signals optimization for the optimal resource allocation problem. Finally, we demonstrate feasibility of this method by applying it to the motivating example - optimal allocation of gas between gas-lifted wells in an oil-production system.

The paper is organized as follows: Section II presents the motivating example. In Section III we formulate the problem of dither signals optimization for the case of distributed ESC for multi-agent systems. Section IV contains analysis and a numerical method to solve it. Section V demonstrates application of the proposed solution to the problem of optimal gas allocation for gas-lifted wells. We conclude with Section VI.

II. MOTIVATING EXAMPLE

In oil production, there are cases when oil reservoir pressure is not high enough to guarantee economically reasonable production rates. In this case one employs various methods of artificial lift. One such method is called gas-lift. In this method, compressed gas is injected down into the well.

In the vertical column of the well the gas reduces the density of the fluid, thus reducing the hydrostatic pressure at the inflow section of the well. This leads to increase of production rate from the reservoir (higher production rates). The production rate depends on the flow-rate of the injected gas, as well as on reservoir pressure, and fluid composition (ratios of oil, water and gas coming from the reservoir). The dependency of the oil rate on the gas injection rate, called production characteristics, is typically a concave curve ($y = f(u)$) with a unique maximum point u^* , where u is gas injection rate and y is the oil production rate. Examples of production curves are given in Figure 3. However, this curve and its maximum are uncertain as they change with slowly varying reservoir conditions and fluid composition. This makes gas-lift a good candidate for model-free optimization methods, like extremum seeking control [12]. Omitting the fluid dynamics from the equation, this optimization problem can be formulated as finding an optimum gas injection rate u^* corresponding to the maximum oil production rate, or maximum of the unknown production characteristic function $f(u)$.

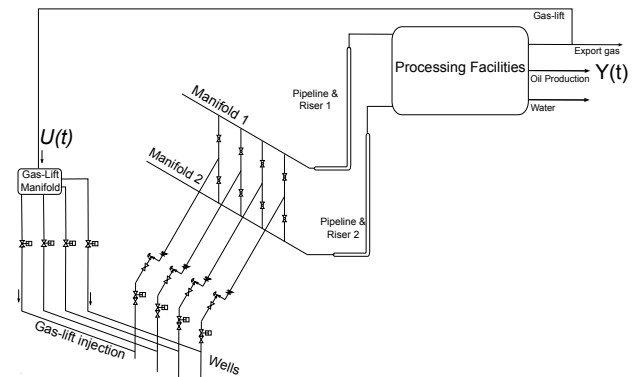


Fig. 1. A production gathering network with 4 gas-lifted wells and subsea manifolds.

In offshore production, there are usually several wells producing to the same top-side processing system and supplied with gas from a common gas compressor, as can be seen in Figure 1. The produced fluids from each well are collected by a subsea manifold and sent to the processing facilities for separation and subsequent exportation. A portion of the gas is pressurized and sent to a gas-lift manifold to be distributed among the wells. For each individual well i , its production characteristic is given by

$$y_i = f_i(u_i), \quad (1)$$

with an uncertain strictly concave function $f_i(u_i)$. In this multi-well setting, the optimization problem becomes the optimal resource (gas) allocation problem: how to distribute the available gas injection rate between individual wells to achieve maximal total oil production from all the wells?

This optimal resource allocation problem has been solved in [12] through distributed perturbation-based ESC algorithm for multi-agent systems. In this approach (as in other

perturbation-based schemes), the injection rate for each individual well equals

$$u_i(t) = \bar{u}_i + d_i(t), \quad (2)$$

and

$$y_i(t) = f_i(\bar{u}_i + d_i(t)), \quad (3)$$

where, for each well i , \bar{u}_i is the quasi static value of the gas injection rate, which is slowly optimized by the ESC, $d_i(t)$ is the dither signal and $y_i(t)$ is the measured oil production rate. The total gas injection rate and oil production rate for all the wells equal

$$U(t) = \sum_{i=1}^N \bar{u}_i + \sum_{i=1}^N d_i(t) \quad (4)$$

$$Y(t) = \sum_{i=1}^N f_i(\bar{u}_i + d_i(t)). \quad (5)$$

Both $U(t)$ and $Y(t)$ consist of slowly varying components (corresponding to \bar{u}_i) and fast changing components corresponding to $d_i(t)$. It is clear from this expression that for a large number of wells, the sum of $d_i(t)$ can result in fast potentially large variations both in the total input and in the total output of the overall production system. These persistent variations constitute a significant load for the compressor and for the top-side processing facilities. However, as it will be demonstrated in the rest of the paper, a dynamically updated optimal choice of the dither signals $d_i(t)$ can allow us to minimize (and sometimes even totally cancel) these variations both in the total input and in the total output. How to find such optimal dither signals is addressed in the rest of the paper.

III. DITHER SIGNALS OPTIMIZATION

In this section we formulate the problem of extremum seeking control with dither signals optimization. We consider N systems of the form (1) with strictly concave functions $f_i(u_i)$. The inputs u_i can vary within the set

$$u_i^{\min} \leq u_i \leq u_i^{\max}, \quad i = 1, \dots, N \quad (6)$$

for some $u_i^{\max} > u_i^{\min}$. In resource allocation problems, there is an additional constraint on the available resources U^{\max} :

$$\sum_{i=1}^N u_i \leq U^{\max}. \quad (7)$$

The extremum seeking problem is to automatically find the maximum of the sum of the systems outputs:

$$\sum_{i=1}^N f_i(u_i) \rightarrow \max \quad (8)$$

subject to constraints (6) and (7).

In perturbation-based extremum seeking control, this problem is solved by introducing an additional dither signal $d_i(t)$ to the nominal input signal \bar{u}_i in order to estimate the

gradient $\frac{\partial f_i}{\partial u_i}$, as given in (2), with the corresponding outputs in (3).

Next we want to optimize the selection of dither signals. This optimization should not interfere with the convergence of the overall ESC algorithm. The minimum requirement for an ESC algorithm to work is that the dither signals, chosen from a certain family of signals \mathcal{D} , have sufficient persistent variation with an amplitude being sufficiently small to allow gradient estimation algorithm to extract the gradient information, and, sufficiently large to ensure robust gradient estimation with noisy measurements:

$$d_i^{\min} \leq \limsup_{t \rightarrow \inf} |d_i(t)| \leq d_i^{\max} \quad (9)$$

for some positive d_i^{\max} and d_i^{\min} , $i = 1, \dots, N$, where T denotes the process time-span.

Motivated by the example in Section II, we formulate the following dither signals optimization problem: find dither signals $d_i(t)$ from the family \mathcal{D} that minimize the amplitudes of the total variations in the input signals and the total variations in the corresponding systems outputs:

$$J_u = \left| \sum_{i=1}^N d_i(t) \right|^2 \rightarrow \min_{\{d_i(\cdot) \in \mathcal{D}\}}, \quad \forall t \in T \quad (10)$$

$$J_f = \left| \sum_{i=1}^N f_i(\bar{u}_i) - f_i(\bar{u}_i + d_i(t)) \right|^2 \rightarrow \min_{\{d_i(\cdot) \in \mathcal{D}\}}, \quad \forall t \in T \quad (11)$$

subject to constraints (9). Notice that, without loss of generality, the excitation amplitudes are considered in squared form because it will fit our results subsequently.

Depending on practical needs, one can combine the two objective functions in (10) and (11) into one or consider minimization of only one of them, setting an low value upper constraint on the other.

Since $f_i(u)$ in (11) is unknown, we utilize its linear approximation instead:

$$f_i(\bar{u}_i) - f_i(\bar{u}_i + d_i) \approx f_i'(\bar{u}_i) \cdot d_i \quad (12)$$

and for simplicity $f_i'(\bar{u}_i)$ is denoted as $F_i(\bar{u}_i)$. This linear approximation is valid for small dither signals d_i with the requirement of how small they should be captured by Eq. (9). Thus, instead of (11), we want to minimize:

$$J_F = \left| \sum_{i=1}^N F_i(\bar{u}_i) \cdot d_i(t) \right|^2 \rightarrow \min_{\{d_i(\cdot)\}}, \quad \forall t \in T \quad (13)$$

Although in (13) the gradients F_i are still unknown, we can use their estimates obtained by the gradient estimator in extremum seeking algorithm.

A. Problem reformulation

In this subsection we reformulate the general dither signals optimization problem (9), (10), (13), for the case of the

family \mathcal{D} being sinusoidal signals, which are commonly used in extremum seeking control:

$$d_i(t) = \alpha_i \sin(\omega t + \varphi_i), \quad i = 1 \dots N \quad (14)$$

where α_i is the amplitude, ω is the frequency and φ_i is the phase of the signal. We assume that ω is chosen by the design of the ESC controller (to achieve time-scale separation), and focus on optimizing amplitudes α_i and phases φ_i .

The cost functions (10), (13) can be rewritten as:

$$J_u = \left| \sum_{i=1}^N \alpha_i \sin(\omega t + \varphi_i) \right|^2 \rightarrow \min_{\{\alpha_i, \varphi_i\}}, \forall t \in T \quad (15)$$

$$J_F = \left| \sum_{i=1}^N F_i \cdot \alpha_i \sin(\omega t + \varphi_i) \right|^2 \rightarrow \min_{\{\alpha_i, \varphi_i\}}, \forall t \in T \quad (16)$$

This results in an essentially nonlinear and non-convex optimization problem with respect to α_i and φ_i , which is very challenging to solve. To resolve this problem, we re-parameterize dither signals in (14) as described below.

1) *Re-parametrization of dither signals*: The dither signals in (14) can be equivalently parametrized in the following way:

$$d_i(t) = a_i \cdot \sin(\omega t) + b_i \cdot \cos(\omega t), \quad (17)$$

such that parameters a_i and b_i that need to be optimized appear linearly in the dither equation in contrast to the nonlinear relation in (14).

With the re-parametrization the variations of the dither signals and of the corresponding outputs become

$$\sum_{i=1}^N d_i(t) = \left(\sum_{i=1}^N a_i \right) \sin(\omega t) + \left(\sum_{i=1}^N b_i \right) \cos(\omega t) \quad (18)$$

$$\sum_{i=1}^N F_i d_i(t) = \left(\sum_{i=1}^N F_i \cdot a_i \right) \sin(\omega t) + \left(\sum_{i=1}^N F_i \cdot b_i \right) \cos(\omega t) \quad (19)$$

2) *Overall dither signal effects*: With the new parametrization of dither signals, the total overall excitation effects can be rewritten. The squared amplitude of the total input variation J_u in Eq.(15) becomes:

$$J_u = \left(\sum_{i=1}^N a_i \right)^2 + \left(\sum_{i=1}^N b_i \right)^2 \quad (20)$$

and the squared amplitude of the total output variation J_F in (16) equals

$$J_F = \left(\sum_{i=1}^N F_i \cdot a_i \right)^2 + \left(\sum_{i=1}^N F_i \cdot b_i \right)^2 \quad (21)$$

Further, the squared amplitude of individual dither signals ($|d_i|$) are written as follows:

$$|d_i(t)|^2 = a_i^2 + b_i^2, \forall t \in T \quad (22)$$

3) *Formulation of the dither signals optimization problem*: With expressions (20)-(22) we can now formulate the problem of finding the optimal parameters a_i and b_i for the dither signals in (17). For clarity, we select to minimize the dither effects on the output (objective (13)), while limiting the amplitude of the total dither signal by δ_{in} (instead of objective function (10)).

Then the dither signal optimization problem is formulated as follows:

$$J_F = \left(\sum_{i=1}^N F_i \cdot a_i \right)^2 + \left(\sum_{i=1}^N F_i \cdot b_i \right)^2 \rightarrow \min_{\{a_i, b_i\}} \quad (23)$$

$$\left(\sum_{i=1}^N a_i \right)^2 + \left(\sum_{i=1}^N b_i \right)^2 \leq \delta_{in}^2 \quad (24)$$

$$(d_i^{min})^2 \leq a_i^2 + b_i^2 \leq (d_i^{max})^2, \quad i = 1 \dots N \quad (25)$$

This is a nonlinear programming problem with a quadratic objective and convex constraints, except for the non-convexity present in the lower bound in (25). Despite this non-convexity, it can be solved efficiently at each time step. To ensure continuity of the input signals, the changes in the parameters of the dither signals (a_i and b_i) from one step to the next step are required to be bounded:

$$|\Delta a_i|^2 \leq \Delta a_i^{max}, \quad i = 1, \dots, N \quad (26)$$

$$|\Delta b_i|^2 \leq \Delta b_i^{max}, \quad i = 1, \dots, N \quad (27)$$

where Δa_i^{max} (Δb_i^{max}) are the maximal admissible changes in a_i (b_i) in consecutive time steps.

In what follows, the dither signal optimizer is incorporated into a distributed extremum-seeking scheme. Since the gradients F_i are unknown, the scheme contains a gradient estimator, which provides estimates \hat{F}_i to both the dither signal optimizer and to a steady-state optimizer. On a faster time-scale, the dither optimizer calculates excitations that are sufficient for gradient estimation and also minimize the total variations in the plant. On a slower time-scale, the steady-state optimizer performs adaptations in the input signals towards the optimal solution also based on the gradient estimates.

IV. DISTRIBUTED ESC WITH DITHER OPTIMIZATION

We propose a distributed extremum-seeking scheme in which the steady-state optimizer is based on gradients synchronization [12], and the gradient estimation is performed with least-squares (LS) fits from past data [5].

The proposed scheme is illustrated in Figure 2. For the static plants considered in this paper, there are two time-scales in the scheme: the fast time scale of dither signal excitations, and the slow time scale of the steady-state optimizer. For a given input signal u_i , the controller measures the corresponding output y_i for the unknown cost function $f_i(u_i)$. Both the input u_i and the system output y_i are sent to the gradient estimator, which calculates the estimated gradient $\frac{\partial \hat{f}_i}{\partial u_i}$ based on a least-squares fit from past data. The gradient estimate is then sent to both the steady-state

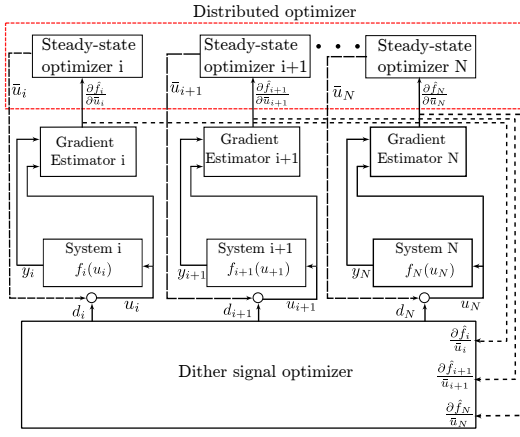


Fig. 2. Extremum-Seeking Scheme.

optimizer and the dither signal optimizer. On a slower time-scale, the steady-state optimizer performs the adaptation of the input signal \bar{u}_i based on a control law derived from the synchronization of gradients from all the systems [12]. On the faster time-scale, the dither signal optimizer solves the optimization problem formulated in Eqs (23)–(27) to determine optimal excitations d_i to each system's input. Finally, the resulting input signal u_i becomes the summation of the nominal input \bar{u}_i and the dither signal d_i received from the dither signal optimizer.

The other systems $j = i + 1, \dots, N$ work analogously. Each system receives the excitations from the dither optimizer on a fast time-scale and performs adaptations of the input signals based on the synchronization the estimated gradients $\frac{\partial \hat{f}_j}{\partial \bar{u}_j}, \forall j \neq i$ on the slow time-scale.

A. Least-squares filter

The gradient estimation has a central role in the ESC scheme since both the dither signal optimizer and the steady-state optimizer rely on accurate gradient estimates to function properly. Many perturbation-based ESC schemes utilize dynamic estimators such as band-pass filters [17] and observers [18] for gradient estimation. In order to avoid the interplay between the dither signal excitations and the estimation, we chose to use a static filter for gradient estimation.

The static estimator works as follows. There is a sliding window that stores data from the last T_w seconds of previous time steps. The gradient is obtained from 1st-order least-square fits $p_i \cdot u_i(t) + q_i$ of window data at time t , which are calculated from the following convex optimization problem:

$$\min_{p_i, q_i} \int_{-T_w}^0 (f_i(t + \tau) - (p_i \cdot u(t + \tau) + q_i))^2 \cdot d\tau \quad (28)$$

The explicit solution for the estimated gradient p_i can be computed in closed-form [5]. The window size T_w is selected to be an integer multiplier of the dither signal wave period. Its size is an important tuning parameter of the estimator, and should be chosen based on the trade-off between the smoothness of the gradient estimates and the delay of the

estimates: the bigger the window size, the smoother and more delayed is the estimation.

B. Synchronization-based optimizer

The steady-state optimizer is responsible for the continuous adaptation of the nominal inputs \bar{u}_i towards the optimum. We chose to utilize the synchronization-based optimizer proposed in [12]. In resource allocation problems with inequality coupling constraints (7), a slight modification in the problem formulation is required. A fictitious input u_{N+1} denoting the slack of the shared resource is created such that $u_{N+1} = U^{\max} - \sum_{i=1}^N u_i$ and its corresponding fictitious function $f_{N+1}(u_{N+1})$ is set to zero. The optimizer is designed based on the optimality condition, which is that the gradients from all systems must be synchronized at the optimal point \mathbf{u}^* :

$$\frac{\partial \hat{f}_i}{\partial u_i}(u_i^*) = \frac{\partial \hat{f}_j}{\partial u_j}(u_j^*), \forall i, j = 1, \dots, N + 1 \quad (29)$$

Each steady-state optimizer is then constructed based on the following synchronization-based control law:

$$\dot{u}_i = \nu \sum_{j \neq i} \gamma_{i,j} \left(\frac{\partial \hat{f}_i}{\partial u_i}(u_i) - \frac{\partial \hat{f}_j}{\partial u_j}(u_j) \right), \quad (30)$$

where the tuning parameters $\gamma_{i,j} = \gamma_{j,i} \geq 0$ and ν are the synchronization gains and optimizer gain respectively. The derivations and convergence proofs of the synchronization-based optimizer applied to a resource allocation problem can be found in [12].

C. Dither signal optimizer

With the estimated gradients \hat{F}_i , the dither signal optimizer defined in Eqs (23)–(27) is formulated as:

$$\hat{J}_F = \left(\sum_{i=1}^N \hat{F}_i \cdot a_i \right)^2 + \left(\sum_{i=1}^N \hat{F}_i \cdot b_i \right)^2 \rightarrow \min_{\{a_i, b_i\}} \quad (31)$$

$$\left(\sum_{i=1}^N a_i \right)^2 + \left(\sum_{i=1}^N b_i \right)^2 \leq \delta_{\text{in}}^2 \quad (32)$$

$$(d_i^{\min})^2 \leq a_i^2 + b_i^2 \leq (d_i^{\max})^2, \quad i = 1 \dots N \quad (33)$$

$$|\Delta a_i| \leq \Delta a^{\max}, \quad i = 1, \dots, N, \quad (34)$$

$$|\Delta b_i| \leq \Delta b^{\max}, \quad i = 1, \dots, N, \quad (35)$$

where \hat{J}_F is the total estimated output variation in the plant.

V. SIMULATIONS

The proposed method is assessed in the gas-lift allocation optimization problem described in Section II.

We consider a production gathering network of $N = 5$ gas-lifted wells. Let $u_i, i = 1, \dots, 5$ be the gas-lift injection rate for each well. The production curves mapping the gas injection rates to corresponding oil production rates are given

by the following functions:

$$f_1(u_1) = -3.9 \times 10^{-7}u_1^4 + 2.1 \times 10^{-4}u_1^3 - 0.043u_1^2 + 3.7u_1 + 12, \quad (36)$$

$$f_2(u_2) = -1.3 \times 10^{-7}u_2^4 + 10^{-4}u_2^3 - 2.8 \times 10^{-2}u_2^2 + 3.1u_2 - 17, \quad (37)$$

$$f_3(u_3) = -1.2 \times 10^{-7}u_3^4 + 10^{-4}u_3^3 - 0.028u_3^2 + 2.5u_3 - 16, \quad (38)$$

$$f_4(u_4) = -4 \times 10^{-7}u_4^4 + 1.8 \times 10^{-4}u_4^3 - 0.036u_4^2 + 3.5u_4 + 10, \quad (39)$$

$$f_5(u_5) = -1.4 \times 10^{-7}u_5^4 + 10^{-4}u_5^3 - 0.029u_5^2 + 3u_5 - 5. \quad (40)$$

The production curves are depicted in Figure 3. The maximum of the curves lies at $(u_1^*, u_2^*, u_3^*, u_4^*, u_5^*) \approx (83.75, 98.31, 64.81, 108.62, 79.68)$. Box constraints are im-

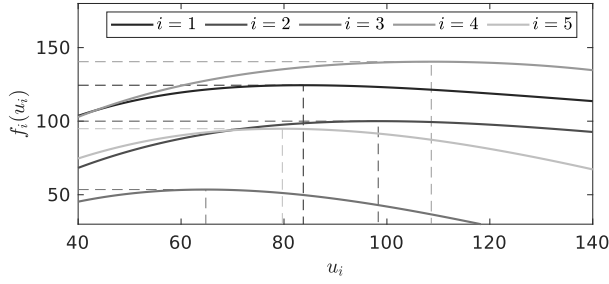


Fig. 3. Gas-lift performance curves.

posed to bound the individual gas injection rates between lower ($u_i^{\min} = 40$) and upper limits ($u_i^{\max} = 140$). Although the proposed ESC scheme is capable of handling constraints, since this is not the focus of this work, we consider a scenario in which the total gas is sufficient to reach the optimal injection rate for all wells, i.e., $U^{\max} \geq u_1^* + u_2^* + u_3^* + u_4^* + u_5^* = 435.17$.

The tuning parameters of the extremum-seeking controllers are set to $\nu = 0.3$, $\omega_i = 0.75$, and $\gamma_{i,j} = 1$, $\forall i, j \in 1, \dots, N$ with $i \neq j$. The initial conditions for the input signals are $u_1(0) = 50$, $u_2(0) = 70$, $u_3(0) = 100$, $u_4(0) = 70$, and $u_5(0) = 50$.

The ESC scheme was implemented in Simulink and Matlab R2018b. The least-squares gradient estimator and the dither signal optimizer are external scripts embedded in the ESC scheme implemented in Simulink. In order to avoid an algebraic loop at time step k , the dither signal optimizer utilizes gradient estimates from time step $k - 1$. The time step was set to $T_s = 0.1$, and the window size for the least squares fits is $T_w = \lceil 3 \times (2\pi/\omega_i)/T_s \rceil$, which corresponds to 3 times the period of the dither signals. The dither signal optimizer is formulated in CasADI v3.4.5 [19], and the dither optimization problem is solved with the nonlinear solver IPOPT [20] at each time step. The bounds for the constraints are set to $\delta_{\text{in}} = 10^{-6}$, $d_i^{\min} = 0.5$, $d_i^{\max} = 2.5$, $\Delta a_i^{\max} = \Delta b_i^{\max} = 0.8$.

To evaluate the performance of the dither signal optimizer, the ESC scheme with dynamically optimized signals is compared to a similar scheme with fixed dither signals. In the latter, the dither signals have the same amplitude and phases, $\alpha_i = 2.5$ and $\phi_i = 0$, $\forall i = 1, \dots, N$.

The total variations in the input signals are shown in Figure 4. While the total variations using dynamically op-

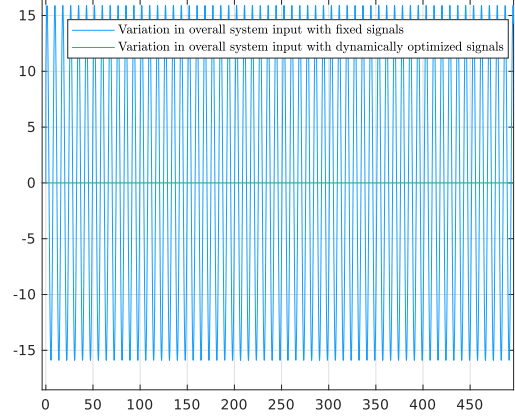


Fig. 4. Dither-induced variations in the total gas injection rate for optimized and fixed dither signals.

timized dither signals J_U is practically zero, the total variations $J_{U,\text{std}}$ with constant dither signals is relatively large, corresponding to a variation in the range of 5 to 10% of the total input. This variation in the fast time-scale can be damaging for the gas-lift compressor and other equipment in the processing facilities.

The resulting gas injection rates u_i , $i = 1, \dots, N$ obtained with the proposed dither optimization scheme are depicted in Figure 5. It can be seen that the injection rates converge to the

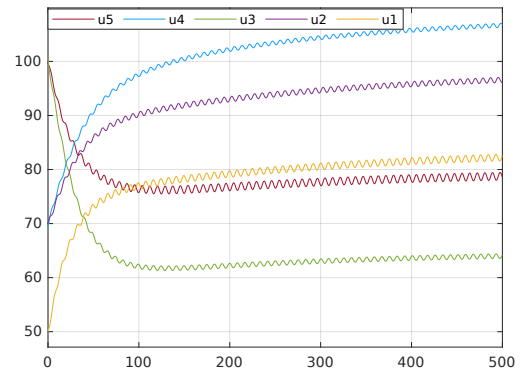


Fig. 5. Input signals.

local neighborhood of the optimal values $(u_1^*, u_2^*, u_3^*, u_4^*, u_5^*) \approx (83.75, 98.31, 64.81, 108.62, 79.68)$.

Figure 6 shows the total oil production rate obtained with dynamically optimized dither signals and, for comparison, for fixed dither signals. As the gas injection rates approach

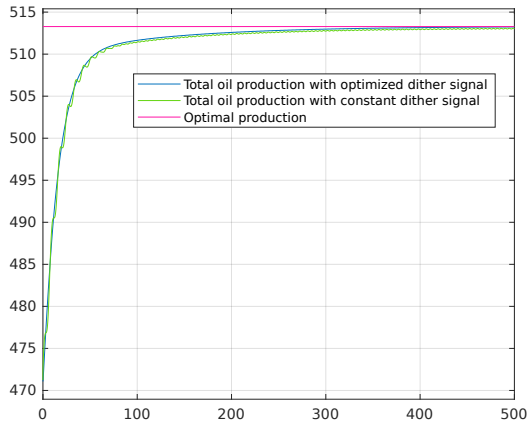


Fig. 6. Objective function.

the optimal solution, the objective function converges to a value that is close to the optimal value $\sum_{i=1}^N f_i(u_i^*) = 513.28$. Notice that the ESC scheme with optimized dither signals has a similar performance to the scheme with constant signals regarding convergence to optimality. However, the latter has more high-frequency variations than the scheme with optimized dither signals because of dither-induced variations in the output. To highlight these differences, we compare the total output variations of both schemes in Figure 7. With optimized signals, the estimated total variation in the

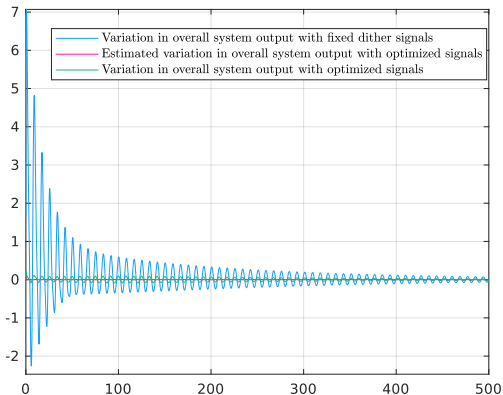


Fig. 7. Dither-induced variations in the total oil production rate for optimized and fixed dither signals.

output \hat{J}_F is practically zero, while the total variation J_F is quite small, bounded by 10^{-2} in absolute values. On the other hand, the total variations with fixed signals, $J_{F,\text{std}}$, is considerably larger, specially during the transients where the gradients are still not synchronized.

To demonstrate adaptation of the sinusoidal dither signals, we demonstrate their amplitudes and phases in Figures 8 and 9. They are calculated from a_i and b_i according to the

following formulas:

$$\alpha_i = \sqrt{a_i^2 + b_i^2} \quad (41)$$

$$\varphi_i = \arctan \frac{b_i}{a_i} \quad (42)$$

The adaptations occur mainly during the transients, when the

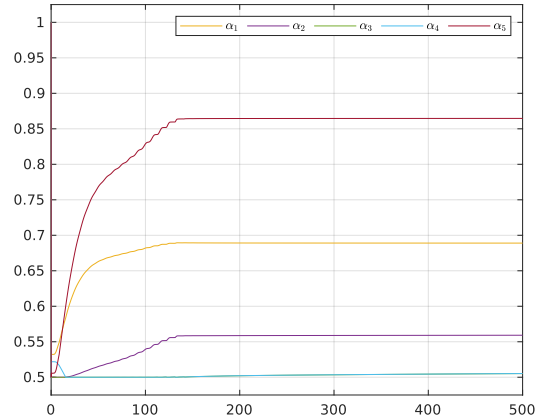


Fig. 8. Signal amplitudes.

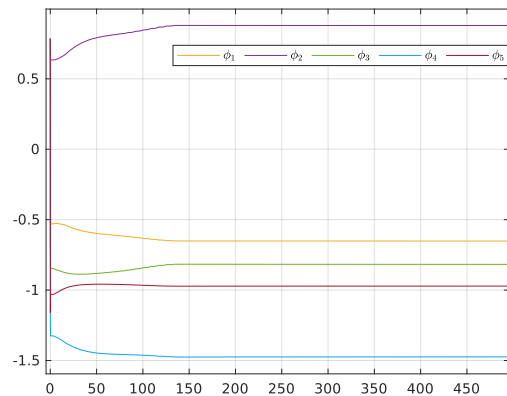


Fig. 9. Signal phases.

total variation tends to be larger. The smoothness of the adaptations depend on the upper bounds chosen for the continuity constraints in Eqs 26 and 27, since these constraints limit the changes in amplitudes and phases between consecutive time steps. The limits for these constraints should be compatible with the gains chosen for the steady-state optimizers.

VI. CONCLUDING REMARKS

In this paper we have presented a perturbation-based extremum-seeking scheme with adaptive dither signals for an optimal resource allocation problem. The adaptation of the dither signals is performed by a dynamic optimizer that minimizes the total variations in the input and output of the plant. The dither optimizer is combined with a distributed

extremum-seeking algorithm based on synchronization of gradients and with a gradient estimator based on least-squares fits. As demonstrated in an example from the petroleum industry, this overall ESC scheme demonstrates the ability to converge to the optimum with similar performance as with fixed dither signals. At the same time, it significantly reduces dither-induced variations in the overall input and output of the system. This feature is particularly attractive for practitioners who are interested in the application of extremum-seeking control in large-scale industrial cases, where the total variations can be prohibitively large.

To the best of the authors' knowledge, this is the first time the problem of dither signals optimization/coordination for multi-agent extremum seeking control systems is formulated and addressed in the literature. Formal stability/convergence proofs, as well as further attempts to simplify the solution will be presented in a journal version of the paper. Further work will also focus on different formulations of the dither optimization problem, which would result in more computationally attractive solutions (e.g. avoiding non-convex optimization problems).

REFERENCES

- [1] M. Krstic and H.-H. Wang, "Stability of extremum seeking feedback for general nonlinear dynamic systems," *Automatica*, vol. 36, no. 4, pp. 595 – 601, 2000.
- [2] K. B. Ariyur and M. Krstic, *Real-time optimization by extremum-seeking control*. John Wiley & Sons, 2003.
- [3] M. Krstic, "Performance improvement and limitations in extremum seeking control," *Systems & Control Letters*, vol. 39, no. 5, pp. 313 – 326, 2000.
- [4] M. Guay and D. Dochain, "A time-varying extremum-seeking control approach," *Automatica*, vol. 51, pp. 356 – 363, 2015.
- [5] B. Hunnekens, M. Haring, N. van de Wouw, and H. Nijmeijer, "A dither-free extremum-seeking control approach using 1st-order least-squares fits for gradient estimation," in *53rd IEEE Conference on Decision and Control*. IEEE, 2014, pp. 2679–2684.
- [6] Y. Tan, D. Nei, and I. Mareels, "On the choice of dither in extremum seeking systems: A case study," *Automatica*, vol. 44, no. 5, pp. 1446 – 1450, 2008.
- [7] Y. Tan, W. H. Moase, C. Manzie, D. Nei, and I. M. Y. Mareels, "Extremum seeking from 1922 to 2010," in *Proceedings of the 29th Chinese Control Conference*, July 2010, pp. 14–26.
- [8] M. A. M. Haring, "Extremum-seeking control: convergence improvements and asymptotic stability," Ph.D. dissertation, NTNU, 2016.
- [9] M. Ye and G. Hu, "A distributed extremum seeking scheme for networked optimization," in *2015 54th IEEE Conference on Decision and Control (CDC)*, Dec 2015, pp. 4928–4933.
- [10] D. Wang, M. Chen, and W. Wang, "Distributed extremum seeking for optimal resource allocation and its application to economic dispatch in smart grids," *IEEE Transactions on Neural Networks and Learning Systems*, vol. 30, no. 10, pp. 3161–3171, Oct 2019.
- [11] J. Ebegbulem and M. Guay, "Resource allocation for a class of multi-agent systems with unknown dynamics using extremum seeking control," in *2018 IEEE Conference on Decision and Control (CDC)*, Dec 2018, pp. 2496–2501.
- [12] A. Pavlov, M. Haring, and K. Fjalestad, "Practical extremum-seeking control for gas-lifted oil production," in *Decision and Control (CDC), 2017 IEEE 56th Annual Conference on*. IEEE, Dec 2017, pp. 2102–2107.
- [13] M. Chioua, B. Srinivasan, M. Guay, and M. Perrier, "Performance improvement of extremum seeking control using recursive least square estimation with forgetting factor," *IFAC-PapersOnLine*, vol. 49, no. 7, pp. 424 – 429, 2016.
- [14] M. Guay, "Proportional-integral extremum-seeking control," *IFAC-PapersOnLine*, vol. 48, no. 8, pp. 675 – 680, 2015.
- [15] R. Suttner, "Extremum seeking control with an adaptive dither signal," *Automatica*, vol. 101, pp. 214 – 222, 2019.
- [16] L. Wang, S. Chen, and K. Ma, "On stability and application of extremum seeking control without steady-state oscillation," *Automatica*, vol. 68, pp. 18 – 26, 2016.
- [17] M. Krstić and H.-H. Wang, "Stability of extremum seeking feedback for general nonlinear dynamic systems," *Automatica*, vol. 36, no. 4, pp. 595–601, 2000.
- [18] M. Haring and T. A. Johansen, "Asymptotic stability of perturbation-based extremum-seeking control for nonlinear plants," *IEEE Transactions on Automatic Control*, vol. 62, no. 5, pp. 2302–2317, 2016.
- [19] J. A. E. Andersson, J. Gillis, G. Horn, J. B. Rawlings, and M. Diehl, "CasADi – A software framework for nonlinear optimization and optimal control," *Mathematical Programming Computation*, vol. 11, no. 1, pp. 1–36, 2019.
- [20] A. Wächter and L. T. Biegler, "On the implementation of an interior-point filter line-search algorithm for large-scale nonlinear programming," *Mathematical Programming*, vol. 106, no. 1, pp. 25–57, Mar 2006.